

RTMW: Real-Time Multi-Person 2D and 3D Whole-body Pose Estimation

Tao Jiang* Xincheng Xie* Yining Li

Shanghai AI Laboratory

{jiangtao, xiexinchen, liyining}@pjlab.org.cn

Abstract

Whole-body pose estimation is a challenging task that requires simultaneous prediction of keypoints for the body, hands, face, and feet. Whole-body pose estimation aims to predict fine-grained pose information for the human body, including the face, torso, hands, and feet, which plays an important role in the study of human-centric perception and generation and in various applications. In this work, we present RTMW (Real-Time Multi-person Whole-body pose estimation models), a series of high-performance models for 2D/3D whole-body pose estimation. We incorporate RTMPose model architecture with FPN and HEM (Hierarchical Encoding Module) to better capture pose information from different body parts with various scales. The model is trained with a rich collection of open-source human keypoint datasets with manually aligned annotations and further enhanced via a two-stage distillation strategy. RTMW demonstrates strong performance on multiple whole-body pose estimation benchmarks while maintaining high inference efficiency and deployment friendliness. We release three sizes: m/l/x, with RTMW-l achieving a 70.2 mAP on the COCO-Wholebody benchmark, making it the first open-source model to exceed 70 mAP on this benchmark. Meanwhile, we explored the performance of RTMW in the task of 3D whole-body pose estimation, conducting image-based monocular 3D whole-body pose estimation in a coordinate classification manner. We hope this work can benefit both academic research and industrial applications. The code and models have been made publicly available at: <https://github.com/open-mmlab/mmpose/tree/main/projects/rtmpose>

1. Introduction

Whole-body pose estimation is an essential component in advancing the capabilities of human-centric artificial intelligence systems. It can be utilized in human-computer interaction, virtual avatar animation, and the film indus-

try. In the context of AIGC (AI Generated Content) applications, the outcomes of whole-body pose estimation are also employed to control character generation. As the emergence of downstream tasks and industrial applications empowered by whole-body pose estimation, designing a model that is highly accurate, low-latency, and easy to deploy is extremely valuable.

In early research on human pose estimation, due to the complexity of the task and limitations in computational power and data, researchers divided the human body into separate parts for independent pose estimation studies. With the relentless efforts of predecessors, remarkable results have been achieved in these singular, part-specific 2D pose estimation tasks.

Previous work, such as OpenPose [3], could obtain whole-body pose estimation results by combining the outcomes of these separate parts. However, this straightforward combination approach faced high computational costs and significant performance limitations. While lightweight tools like MediaPipe [22] offer high real-time performance and ease of deployment, their accuracy is not entirely satisfactory.

Our MMPose [5] team released the RTMPose [10] model last year, which achieved an excellent balance between accuracy and real-time performance. Subsequently, on this foundation, DWPose [40] further enhanced the performance of RTMPose in whole-body pose estimation tasks by incorporating a two-stage distillation technique and integrating a new dataset, UBody [17].

The structural design of RTMPose [10] initially only considered the body posture. However, in whole-body pose estimation tasks, feature resolution is crucial for accuracy in facial, hand, and foot pose estimation. Therefore, we introduced two techniques, PAFPN (Part-Aggregation Feature Pyramid Network) and HEM (High-Efficiency Multi-Scale Feature Fusion), to enhance feature resolution. Experimental results have confirmed that these two modules significantly improve the localization accuracy of fine-grained body parts.

At the same time, the scarcity of open-source whole-body pose estimation datasets greatly limits the perfor-

* Equal Contribution.

mance of open-source models. To fully use datasets focusing on different body parts, we manually aligned the key point definitions of 14 open-source datasets (3 for whole-body keypoints, 6 for body keypoints, 4 for facial keypoints, and 1 for hand keypoints), which are jointly used to train RTMW.

In the realm of 3D whole-body pose estimation, the academic community has predominantly embraced two main methodologies: Lifting [26, 29, 42] and regression [28, 32] approaches. There has been a notable absence of scholarly inquiry into methods grounded in the SimCC [16] technique. Our research endeavors have ventured into uncharted territory by applying the RTMW architecture to the 3D whole-body pose estimation task. Our experimental findings indicate that the SimCC [16] method holds its own and delivers commendable performance in this domain.

2. Related Work

Top-down Approaches. Top-down algorithms use off-the-shelf detectors to provide bounding boxes and crop the human to a uniform scale for pose estimation. Algorithms [2, 18, 31, 37, 39] of the top-down paradigm have dominated public benchmarks. The two-stage inference paradigm allows both the human detector and the pose estimator to use relatively small input resolutions, allowing them to outperform bottom-up algorithms in speed and accuracy in non-extreme scenarios (i.e. when the number of people in the image is no more than 6). Additionally, most previous work has focused on achieving state-of-the-art performance on public datasets. In contrast, our work aims to design models with better speed-accuracy trade-offs to meet the needs of industrial applications.

Coordinate Classification. Previous pose estimation approaches usually regard keypoint localization as either coordinate regression (e.g. [14, 25, 33]) or heatmap regression (e.g. [8, 37, 39, 41]). SimCC [16] introduces a new scheme that formulates keypoint prediction as classification from sub-pixel bins for horizontal and vertical coordinates respectively, which brings about several advantages. First, SimCC is freed from the dependence on high-resolution heatmaps, thus allowing for a very compact architecture that requires neither high-resolution intermediate representations [31] nor costly upscaling layers [37]. Second, SimCC flattens the final feature map for classification instead of involving global pooling [33] and, therefore, avoids the loss of spatial information. Third, the quantization error can be effectively alleviated by coordinate classification at the sub-pixel scale without needing extra refinement post-processing [41]. These qualities make SimCC attractive for building lightweight pose estimation models. RTMO [21] introduced the coordinate classification method

into the one-stage pose estimation, which has achieved significant performance improvement and also confirmed the great potential of the SimCC method in pose estimation tasks. In this work, we further exploit the coordinate classification scheme with optimizations on model architecture and training strategy.

3D pose estimation 3D pose estimation is a vibrant research domain with extensive industry applications. The landscape of contemporary methodologies is dominated by two primary approaches: lifting methods [26, 29, 42] that leverage 2D keypoints and regression methods grounded in image analysis. The lifting methods, which input 2D coordinates into a neural network to directly predict their spatial coordinates, are distinguished by their swift computational pace. However, this efficiency comes at the cost of scene information, as these algorithms are devoid of image input, leading to a reliance on the annotation of training data for the range of their predictive outcomes.

Conversely, image-based regression methods [28, 32], while incorporating rich visual data, face the challenges of sluggish inference speeds and increased task complexity. These factors contribute to difficulty in training the models and achieving high accuracy. Our proposed method, RTMW3D, diverges from these conventional approaches by employing a classification strategy based on the Simcc technique [16] to refine the final spatial coordinates through post-processing. Our experimental findings underscore the effectiveness of this innovative approach.

3. Model Architecture and Training

Although the RTMPose we proposed before did not have a special design for the whole-body keypoint estimation task, after experiments, we found that its performance is comparable to the current state-of-the-art method, ZoomNas [38]. However, during the experimental process, we found that RTMPose has a certain performance bottleneck in the whole-body pose estimation task. As the scale of parameters increases, the model performance does not improve with the increase in the number of parameters. On the other hand, with the research of other research teams, such as the DWPose team, although they added new datasets during the training of RTMPose and adopted more efficient two-stage distillation training technology, which effectively improved the accuracy of RTMPose, they still cannot avoid the problem of the inherent performance bottleneck of RTMPose as the number of parameters increases.

3.1. RTMW

3.1.1 Task Limitation

We first analyze some of the unsolved problems in the whole-body pose estimation task. RTMW was designed to

address these challenges. The first issue is the resolution limit of local areas. In an image, parts of the human body, such as the face, hands, and feet, occupy a very small proportion of the human body and the image. For a model, the input resolution of these areas will directly affect the accuracy of the model’s prediction of the keypoints in these parts. The second problem is that the difficulty of learning keypoints from different human body parts varies. For example, the keypoints on the face can be regarded as some points attached to the face, a rigid body, and since the deformation of the face is very small, the model will find it easier to learn to predict these facial keypoints. On the contrary, hand keypoints have a higher degree of freedom due to the rotation and movement of the fingers and wrists, making them much more difficult to predict. The third problem lies in the loss function. Commonly used loss functions such as the KL divergence and the regression error are calculated point-by-point. Thus, they tend to be dominated by body parts with more keypoints and larger spatial proportions, like the torso and face, paying insufficient attention to small but complex parts like hands and feet. This typically results in imbalanced convergence, meaning the model archives lower average error but exhibits poor accuracy on complex body parts. The last point is that there are very few open-source whole-body pose estimation datasets, significantly limiting our research on the model’s capabilities. In response to the above limitations, we have designed a set of targeted optimization solutions for RTMPose and proposed our RTMW model.

3.1.2 Model Architecture

The RTMW model structure is shown in Figure 1, designed based on RTMPose, incorporating PAFPN [19] and HEM modules to enhance feature resolution. Among these, FPN (Feature Pyramid Network) is an effective technique for improving feature resolution and is widely used in the model structures of dense prediction tasks. In addition to this, inspired by the hierarchical encoding concept proposed in the VQVAE-2 [30] paper, we introduced a HEM (Hierarchical Encoding Module) module. Experimental results show that the simultaneous introduction of these two modules can significantly enhance the performance of RTMPose in whole-body pose estimation tasks.

PAFPN In the previous analysis, since we emphasized the impact of the input resolution of various body parts on the model’s prediction accuracy, we naturally introduced an FPN module. This technique is very common in other vision tasks, such as object detection tasks. Details of this module can be referred to in the original paper [19] and another improved version used in RTMDet [24].

HEM (Hierarchical Encoding Module) The inspiration for this module comes from the work VQVAEv2, which introduced a hierarchical concept on top of the original Encoder-Decoder architecture. In the original VQVAE work, the generated images lacked clear and rich details. Therefore, in the second version, they added hierarchical encoding to features of different resolutions and decoded these hierarchical features separately during the decoding process, which enriched the details in the generated images. We were inspired by this idea in the design of RTMW, creating the HEM (Hierarchical Encoding Module), which performs SimCC encoding on the features output by PAFPN in a hierarchical manner, then merges them after the hierarchical encoding and finally decodes them in the decoder. Experiments have shown that this design can improve the prediction accuracy of low-resolution body parts in human pose estimation.

3.1.3 Training Techniques

Due to the lack of open-source whole-body pose estimation datasets, we manually aligned 14 open-source datasets that include whole-body, torso, hand, and facial keypoints for pose estimation. We used these 14 datasets for joint training. At the same time, to maximize the model’s performance, we adopted the two-stage distillation technique used by DWPose during the model training process to further enhance the model’s performance.

3.2. RTMW3D

We further explore extending RTMW architecture to 3D whole-body pose estimation, which is challenging due to its ill-posed nature. Specifically, while it is straightforward to ascertain the x and y coordinates of a keypoint from a single RGB image, the ambiguity of the z-axis introduces complexity in the model’s learning process. Furthermore, the scarcity of open-source 3D human pose datasets, especially those with keypoint annotations, and the limited scene diversity of available datasets severely hamper the model’s performance and generalization ability. To address these challenges, RTMW3D has been tailored to excel in monocular 3D pose estimation by refining the 3D dataset, redefining the z-axis, and mitigating the learning difficulty of predicting z-axis coordinates. Structurally, RTMW3D closely mirrors RTMW, with the notable addition of a z-axis prediction branch to the decoder head.

Task definition RTMW3D adheres to the principles of 2D pose estimation, directly forecasting the x and y coordinates of keypoints on the SimCC coordinate space. Following the design of the SimCC [16] method, as shown in figure 2, for the z-axis, we eschew the direct use of annotated z-axis coordinates from the dataset. Instead, we estab-

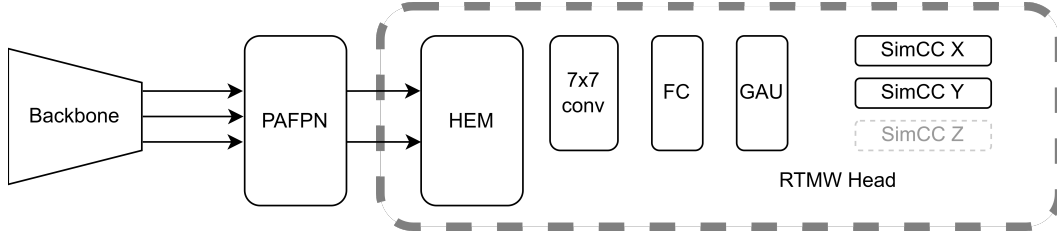


Figure 1. The RTMW arch.

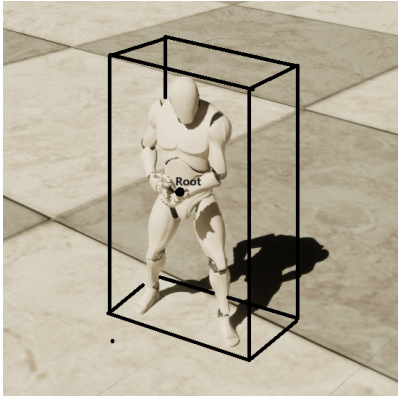


Figure 2. The task definition of 3d pose estimation.

lish a root point for the human skeleton and calculate the z-axis offsets of keypoints relative to this root point. This innovative approach standardizes the z-axis across various datasets and simplifies the model’s learning challenge.

Data process Given the lack of 3D human pose datasets centered on keypoints, we implemented a synergistic training strategy that integrates both 2D and 3D datasets. This approach enriches the data with diverse scenarios, bolstering the model’s performance on 2D pose estimation tasks. To address the issue of the lack of z-axis annotations in 2D keypoint datasets, we have incorporated a z-axis mask into the 2D keypoint data. This modification facilitates a unified training protocol for both data types, enabling the model to accurately predict the x and y coordinates of keypoints and enhance its capacity for 2D pose estimation.

4. Experiments

4.1. Datasets

During the training phase, we continued to use all the training techniques employed in RTMPose and adopted the two-stage distillation technology proposed by DWPose. Due to the limited availability of open-source whole-body pose estimation datasets, we integrated 14 datasets from different parts, manually aligned the keypoint definitions, and uniformly mapped them to the 133-point definition of COCO-Wholebody. In the monocular 3D whole-body

pose estimation task, due to the lack of open-source 3D datasets, we combined 14 existing 2D datasets with three open-source 3D datasets for joint training using a total of 17 datasets. The datasets we used are as follows:

- 3 whole-body datasets: COCO-Wholebody [11, 38], UBody [17], Halpe [6]
- 6 human body datasets: AIC [7], CrowdPose [15], MPII [1], sub-JHMDB [9], PoseTrack18 [37], Human-Art [13]
- 4 face datasets: WFLW [36], 300W, COFW, LaPa [20]
- 1 hand dataset: InterHand [27]
- 3 3D whole-body point datasets: H3WB [43], UBody [17], DNA-rendering [4]

For detailed mapping relationships, please refer to the appendix. We carried out a two-stage distillation of RTMW according to the process proposed by DWPose [40], and the relevant hyperparameters followed the settings in DW-Pose [40].

4.2. Results

COCO-Wholebody We validate the proposed RTMW model on the whole-body pose estimation task with COCO-WholeBody [12, 38] V1.0 dataset. As shown in Table 1, RTMW achieves superior performance and well balances accuracy and complexity. In addition, our proposed RTMW3D also demonstrates good performance on COCO-WholeBody.

H3WB H3WB [43] is currently the only open-source 3D whole-body pose estimation dataset that provides a test set. We evaluated the performance of RTMW3D on the test set of H3WB, and the results are shown in Table 2. Similarly, RTMW3D has achieved excellent performance on the H3WB dataset.

Inference speed As our primary focus is on the development of a real-time model, the inference speed emerges as a critical performance metric. The evaluation of RTMW

Table 1. Whole-body pose estimation results on COCO-WholeBody [12, 38] V1.0 dataset. “*” denotes the model is pre-trained on AIC+COCO. “†” denotes the model is trained on the combined dataset introduced at 4.

	Method	Input Size	whole-body		body		foot		face		hand	
			AP	AR	AP	AR	AP	AR	AP	AR	AP	AR
Top-Down Methods	DeepPose [33]	384×288	33.5	45.6	42.7	58.3	9.9	36.9	64.9	69.7	40.8	58.0
	SimpleBaseline [37]	384×288	57.3	67.1	66.6	74.7	63.5	76.3	73.2	81.2	53.7	64.7
	HRNet [31]	384×288	58.6	67.4	70.1	77.3	58.6	69.2	72.7	78.3	51.6	60.4
	PVT [35]	384×288	58.9	68.9	67.3	76.1	66.0	79.4	74.5	82.2	54.5	65.4
	FastPose50-dcn-si [6]	256×192	59.2	66.5	70.6	75.6	70.2	77.5	77.5	82.5	45.7	53.9
	ZoomNet [11]	384×288	63.0	74.2	74.5	81.0	60.9	70.8	88.0	92.4	57.9	73.4
	ZoomNAS [38]	384×288	65.4	74.4	74.0	80.7	61.7	71.8	88.9	93.0	62.5	74.0
	DWPose-l [40]	384×288	66.5	74.3	72.2	78.9	70.4	81.6	88.7	92.1	62.1	72.0
RTMPose [10]	RTMPose-m*	256×192	58.2	67.4	67.3	75.0	61.5	75.2	81.3	87.1	47.5	58.9
	RTMPose-l*	256×192	61.1	70.0	69.5	76.9	65.8	78.5	83.3	88.7	51.9	62.8
	RTMPose-l*	384×288	64.8	73.0	71.2	78.1	69.3	81.1	88.2	91.9	57.9	67.7
	RTMPose-x*	384×288	65.2	73.2	71.2	78.0	68.1	80.4	89.0	92.2	59.3	68.7
	RTMPose-x*	384×288	65.3	73.3	71.4	78.4	69.2	81.0	88.9	92.3	59.0	68.5
RTMW3D	RTMW3D-l†	384×288	67.8	75.5	74.4	80.7	77.1	86.7	88.2	91.9	61.7	70.6
	RTMW3D-x†	384×288	68.0	75.9	73.9	80.5	76.6	86.8	88.6	92.1	62.7	72.2
RTMW	RTMW-m†	256×192	58.0	67.3	67.6	74.7	67.1	79.4	78.3	85.4	49.1	60.4
	RTMW-l†	256×192	66.2	74.6	74.3	80.7	76.3	86.8	83.4	88.9	59.8	70.1
	RTMW-x†	256×192	67.2	75.2	74.6	80.8	77.0	86.9	84.4	89.6	61.0	71.0
	RTMW-l†	384×288	70.1	78.0	76.1	82.4	79.3	88.5	88.4	92.1	66.3	75.2
	RTMW-x†	384×288	70.2	78.1	76.3	82.6	79.6	88.8	88.4	92.3	66.4	75.5

Table 2. Whole-body 3D pose estimation results on H3WB [43] dataset. “*” denotes the results are borrowed from H3WB paper [43].

Method	Input Size	MPJPE
CanonPose [34] with 3D supervision*	N/A	0.117
Large SimpleBaseline* [37]	N/A	0.112
JointFormer* [23]	N/A	0.088
RTMW3D-l	384x288	0.056
RTMW3D-x	384x288	0.057

models’ inference speed is detailed in the accompanying table 3. Although RTMW, which incorporates an additional module relative to RTMPose, exhibits a marginally reduced inference speed, it offers a substantial enhancement in accuracy. This trade-off is deemed justifiable in the context of our objectives.

Table 3. Inference speed on CPU. RTMPose models are deployed and tested using ONNXRuntime. Flip test is not used in this table.

Results	Input Size	GFLOPs	AP	CPU(ms)	
COCO-WholeBody [11]	HRNet-w32+DARK	256 × 192	7.72	57.8	39.051
	RTMPose-m	256 × 192	2.22	59.1	13.496
	RTMPose-l	256 × 192	4.52	62.2	23.410
	HRNet-w48+DARK	384 × 288	35.52	65.3	150.765
	RTMPose-l	384 × 288	10.07	66.1	44.581
	RTMW-l	256 × 192	7.9	66.0	35.322
	RTMW-l	384 × 288	17.7	70.1	47.618

4.3. Ablation study

4.3.1 Ablation on RTMW

We tested the impact of each module of RTMW on the performance, and the results are shown in table 4. The models are trained on COCO-Wholebody [12, 38], Ubody [17], and Halpe [6] datasets, and the input shape is 256 × 192. The experimental results indicate that the PAFPN and HEM modules we employed can significantly enhance the prediction accuracy, particularly for body parts like hands and feet with lower input resolutions, where the improvement in predictive accuracy is substantial.

4.4. Visualization Results

Figure 3 and Figure 4 present visual representations of the inference outcomes for the RTMW and RTMW3D models. These illustrations demonstrate that the performance of both RTMW and RTMW3D models is commendably high, corroborating the quantitative assessment data.

Table 4. Ablation on RTMW. Models are trained on COCO-WholeBody+UBody+Halpe.

	PAFPN	HEM	GAU	Whole	Body	Foot	Face	Hand
RTMPose-1			✓	63.8	71.7	71.5	83.3	56.4
w/ PAFPN	✓		✓	64.3 (+0.5)	71.8 (+0.1)	71.3 (-0.2)	84.0 (+0.7)	57.7 (+1.3)
w/ HEM		✓	✓	64.1 (+0.3)	72.0 (+0.3)	71.9 (+0.4)	83.4 (+0.1)	57.1 (+0.7)
w/ PAFPN + HEM	✓	✓	✓	65.3 (+1.5)	72.7 (+1.0)	74.8 (+3.3)	84.0 (+0.7)	59.9 (+3.5)
w/o GAU	✓	✓		64.8 (+1.0)	71.9 (+0.2)	72.2 (+0.7)	84.1 (+0.8)	59.5 (+3.1)



Figure 3. 2D visualization results

5. Conclusion

This paper expands the existing scholarly work by critically examining the intricacies and challenges inherent in whole-body pose estimation. Leveraging our established RTMPose model as a foundation, we introduce an enhanced, high-performance model, RTMW/RTMW3D, for real-time whole-body pose estimation. Our model has demonstrated unparalleled performance among all open-source alternatives and possesses a distinct monocular 3D pose estimation capability. We anticipate that the proposed algorithm and its open-source availability will address several practical requirements within the industry for robust pose estimation solutions.

References

- [1] Mykhaylo Andriluka, Leonid Pishchulin, Peter Gehler, and Bernt Schiele. 2d human pose estimation: New benchmark and state of the art analysis. In *IEEE Conference on Computer Vision and Pattern Recognition (CVPR)*, June 2014. 4
- [2] Yuanhao Cai, Zhicheng Wang, Zhengxiong Luo, Binyi Yin, Angang Du, Haoqian Wang, Xiangyu Zhang, Xinyu Zhou, Erjin Zhou, and Jian Sun. Learning delicate local representations for multi-person pose estimation. In *ECCV*, pages 455–472. Springer, 2020. 2



Figure 4. RTMW3D inference results (The 2D and 3D keypoints are both obtained from the RTMW3D model after a single inference.)

- [3] Z. Cao, G. Hidalgo Martinez, T. Simon, S. Wei, and Y. A. Sheikh. Openpose: Realtime multi-person 2d pose estimation using part affinity fields. *IEEE Transactions on Pattern Analysis and Machine Intelligence*, 2019. 1
- [4] Wei Cheng, Ruixiang Chen, Wanqi Yin, Siming Fan, Keyu Chen, Honglin He, Huiwen Luo, Zhongang Cai, Jingbo Wang, Yang Gao, Zhengming Yu, Zhengyu Lin, Daxuan Ren, Lei Yang, Ziwei Liu, Chen Change Loy, Chen Qian, Wayne Wu, Dahua Lin, Bo Dai, and Kwan-Yee Lin. Dna-rendering: A diverse neural actor repository for high-fidelity human-centric rendering. *arXiv preprint*, arXiv:2307.10173, 2023. 4
- [5] MMPose Contributors. Openmmlab pose estimation toolbox and benchmark. <https://github.com/open-mmlab/mmpose>, 2020. 1
- [6] Hao-Shu Fang, Jiefeng Li, Hongyang Tang, Chao Xu, Haoyi Zhu, Yuliang Xiu, Yong-Lu Li, and Cewu Lu. Alphapose: Whole-body regional multi-person pose estimation and tracking in real-time. *IEEE Transactions on Pattern Analysis and Machine Intelligence*, 2022. 4, 5
- [7] Federico Fulgeri, Matteo Fabbri, Stefano Alletto, Simone Calderara, and Rita Cucchiara. Can adversarial networks hallucinate occluded people with a plausible aspect? *arXiv preprint arXiv:1901.08097*, 2019. 4
- [8] Junjie Huang, Zheng Zhu, Feng Guo, and Guan Huang. The devil is in the details: Delving into unbiased data processing for human pose estimation. In *CVPR*, pages 5700–5709, 2020. 2
- [9] H. Jhuang, J. Gall, S. Zuffi, C. Schmid, and M. J. Black. Towards understanding action recognition. In *International Conf. on Computer Vision (ICCV)*, pages 3192–3199, Dec. 2013. 4
- [10] Tao Jiang, Peng Lu, Li Zhang, Ningsheng Ma, Rui Han, Chengqi Lyu, Yining Li, and Kai Chen. RtmPose: Real-time multi-person pose estimation based on mmpose, 2023. 1, 5
- [11] Sheng Jin, Lumin Xu, Jin Xu, Can Wang, Wentao Liu, Chen Qian, Wanli Ouyang, and Ping Luo. Whole-body human pose estimation in the wild, 2020. 4, 5
- [12] Sheng Jin, Lumin Xu, Jin Xu, Can Wang, Wentao Liu, Chen Qian, Wanli Ouyang, and Ping Luo. Whole-body human pose estimation in the wild. In *Proceedings of the European Conference on Computer Vision (ECCV)*, 2020. 4, 5
- [13] Xuan Ju, Ailing Zeng, Jianan Wang, Qiang Xu, and Lei Zhang. Human-art: A versatile human-centric dataset bridging natural and artificial scenes. In *Proceedings of the IEEE/CVF Conference on Computer Vision and Pattern Recognition*, 2023. 4
- [14] Jiefeng Li, Siyuan Bian, Ailing Zeng, Can Wang, Bo Pang, Wentao Liu, and Cewu Lu. Human pose regression with residual log-likelihood estimation. In *ICCV*, 2021. 2
- [15] Jiefeng Li, Can Wang, Hao Zhu, Yihuan Mao, Hao-Shu Fang, and Cewu Lu. Crowdpose: Efficient crowded scenes pose estimation and a new benchmark. *arXiv preprint arXiv:1812.00324*, 2018. 4
- [16] Yanjie Li, Sen Yang, Peidong Liu, Shoukui Zhang, Yunxiao Wang, Zhicheng Wang, Wankou Yang, and Shu-Tao Xia. Simcc: a simple coordinate classification perspective for human pose estimation, 2021. 2, 3
- [17] Jing Lin, Ailing Zeng, Haoqian Wang, Lei Zhang, and Yu Li. One-stage 3d whole-body mesh recovery with component aware transformer. In *Proceedings of the IEEE/CVF Conference on Computer Vision and Pattern Recognition*, pages 21159–21168, 2023. 1, 4, 5
- [18] Huajun Liu, Fuqiang Liu, Xinyi Fan, and Dong Huang. Polarized self-attention: towards high-quality pixel-wise regression. *arXiv preprint arXiv:2107.00782*, 2021. 2
- [19] Shu Liu, Lu Qi, Haifang Qin, Jianping Shi, and Jiaya Jia. Path aggregation network for instance segmentation. In *Proceedings of IEEE Conference on Computer Vision and Pattern Recognition (CVPR)*, 2018. 3
- [20] Yinglu Liu, Hailin Shi, Hao Shen, Yue Si, Xiaobo Wang, and Tao Mei. A new dataset and boundary-attention semantic segmentation for face parsing. In *AAAI*, pages 11637–11644, 2020. 4
- [21] Peng Lu, Tao Jiang, Yining Li, Xiangtai Li, Kai Chen, and Wenming Yang. RTMO: Towards high-performance one-stage real-time multi-person pose estimation, 2023. 2
- [22] Camillo Lugaresi, Jiuqiang Tang, Hadon Nash, Chris McClanahan, Esha Uboweja, Michael Hays, Fan Zhang, Chuoling Chang, Ming Guang Yong, Juhyun Lee, Wan-Teh Chang, Wei Hua, Manfred Georg, and Matthias Grundmann. Mediapipe: A framework for building perception pipelines, 2019. 1
- [23] Sebastian Lutz, Richard Blythman, Koustav Ghostal, Moynihan Matthew, Ciaran Simms, and Aljosa Smolic. Jointformer: Single-frame lifting transformer with error prediction and refinement for 3d human pose estimation. *26TH International Conference on Pattern Recognition, ICPR 2022*, 2022. 5
- [24] Chengqi Lyu, Wenwei Zhang, Haian Huang, Yue Zhou, Yudong Wang, Yanyi Liu, Shilong Zhang, and Kai Chen. RtmDET: An empirical study of designing real-time object detectors, 2022. 3
- [25] Weian Mao, Yongtao Ge, Chunhua Shen, Zhi Tian, Xinlong Wang, Zhibin Wang, and Anton van den Hengel. Poseur: Direct human pose regression with transformers. In *European Conference on Computer Vision*, pages 72–88. Springer, 2022. 2
- [26] Julieta Martinez, Rayat Hossain, Javier Romero, and James J. Little. A simple yet effective baseline for 3d human pose estimation. In *ICCV*, 2017. 2
- [27] Gyeongsik Moon, Shoou-I Yu, He Wen, Takaaki Shiratori, and Kyoung Mu Lee. Interhand2.6m: A dataset and baseline for 3d interacting hand pose estimation from a single rgb image. In *European Conference on Computer Vision (ECCV)*, 2020. 4
- [28] Georgios Pavlakos, Xiaowei Zhou, Konstantinos G Derpanis, and Kostas Daniilidis. Coarse-to-fine volumetric prediction for single-image 3D human pose. In *Computer Vision and Pattern Recognition (CVPR)*, 2017. 2
- [29] Dario Pavullo, Christoph Feichtenhofer, David Grangier, and Michael Auli. 3d human pose estimation in video with temporal convolutions and semi-supervised training. In *Conference on Computer Vision and Pattern Recognition (CVPR)*, 2019. 2

- [30] Ali Razavi, Aaron van den Oord, and Oriol Vinyals. Generating diverse high-fidelity images with vq-vae-2, 2019. 3
- [31] Ke Sun, Bin Xiao, Dong Liu, and Jingdong Wang. Deep high-resolution representation learning for human pose estimation. In *CVPR*, 2019. 2, 5, 6
- [32] Xiao Sun, Bin Xiao, Shuang Liang, and Yichen Wei. Integral human pose regression. *arXiv preprint arXiv:1711.08229*, 2017. 2
- [33] Alexander Toshev and Christian Szegedy. Deeppose: Human pose estimation via deep neural networks. In *Proceedings of the IEEE Conference on Computer Vision and Pattern Recognition (CVPR)*, June 2014. 2, 5
- [34] Bastian Wandt, Marco Rudolph, Petrisa Zell, Helge Rhodin, and Bodo Rosenhahn. Canonpose: Self-supervised monocular 3d human pose estimation in the wild. In *Computer Vision and Pattern Recognition (CVPR)*, June 2021. 5
- [35] Wenhai Wang, Enze Xie, Xiang Li, Deng-Ping Fan, Kaitao Song, Ding Liang, Tong Lu, Ping Luo, and Ling Shao. Pyramid vision transformer: A versatile backbone for dense prediction without convolutions. *arXiv: Computer Vision and Pattern Recognition*, 2021. 5
- [36] Wayne Wu, Chen Qian, Shuo Yang, Quan Wang, Yici Cai, and Qiang Zhou. Look at boundary: A boundary-aware face alignment algorithm. In *CVPR*, 2018. 4
- [37] Bin Xiao, Haiping Wu, and Yichen Wei. Simple baselines for human pose estimation and tracking. In *European Conference on Computer Vision (ECCV)*, 2018. 2, 4, 5
- [38] Lumin Xu, Sheng Jin, Wentao Liu, Chen Qian, Wanli Ouyang, Ping Luo, and Xiaogang Wang. Zoomnas: Searching for whole-body human pose estimation in the wild. *IEEE Transactions on Pattern Analysis and Machine Intelligence*, 2022. 2, 4, 5
- [39] Yufei Xu, Jing Zhang, Qiming Zhang, and Dacheng Tao. Vitpose: Simple vision transformer baselines for human pose estimation, 2022. 2
- [40] Zhendong Yang, Ailing Zeng, Chun Yuan, and Yu Li. Effective whole-body pose estimation with two-stages distillation. In *Proceedings of the IEEE/CVF International Conference on Computer Vision*, pages 4210–4220, 2023. 1, 4, 5, 6
- [41] Feng Zhang, Xiatian Zhu, Hanbin Dai, Mao Ye, and Ce Zhu. Distribution-aware coordinate representation for human pose estimation. In *IEEE/CVF Conference on Computer Vision and Pattern Recognition (CVPR)*, June 2020. 2
- [42] Wentao Zhu, Xiaoxuan Ma, Zhaoyang Liu, Libin Liu, Wayne Wu, and Yizhou Wang. Motionbert: A unified perspective on learning human motion representations. In *Proceedings of the IEEE/CVF International Conference on Computer Vision*, 2023. 2
- [43] Yue Zhu, Nermin Samet, and David Picard. H3wb: Human3.6m 3d wholebody dataset and benchmark. In *Proceedings of the IEEE/CVF International Conference on Computer Vision (ICCV)*, pages 20166–20177, October 2023. 4, 5